Murine AKAP7 Has a 2′,5′-Phosphodiesterase Domain That Can Complement an Inactive Murine Coronavirus ns2 Gene

Elona Gusho,[a,b] Rong Zhang,[c] Babal K. Jha,[a] Joshua M. Thornbrough,[c] Beihua Dong,[a] Christina Gaughan,[a] Ruth Elliott,[c] Susan R. Weiss,[c] Robert H. Silverman[a]

Department of Cancer Biology, Lerner Research Institute, Cleveland Clinic, Cleveland, Ohio, USA[a]; Department of Biological, Geological, and Environmental Sciences, Cleveland State University, Cleveland, Ohio, USA[b]; Department of Microbiology, Perelman School of Medicine, University of Pennsylvania, Philadelphia, Pennsylvania, USA[c]

E.G., R.Z., and B.K.J. contributed equally to this article.

ABSTRACT **Viral 2′,5′-phosphodiesterases (2′,5′-PDEs) help disparate RNA viruses evade the antiviral activity of interferon (IFN) by degrading 2′,5′-oligoadenylate (2-5A) activators of RNase L. A kinase anchoring proteins (AKAPs) bind the regulatory subunits of protein kinase A (PKA) to localize and organize cyclic AMP (cAMP) signaling during diverse physiological processes. Among more than 43 AKAP isoforms, AKAP7 appears to be unique in its homology to viral 2′,5′-PDEs. Here we show that mouse AKAP7 rapidly degrades 2-5A with kinetics similar to that of murine coronavirus (mouse hepatitis virus [MHV]) strain A59 ns2 and human rotavirus strain WA VP3 proteins. To determine whether AKAP7 could substitute for a viral 2′,5′-PDE, we inserted AKAP7 cDNA into an MHV genome with an inactivated ns2 gene. The AKAP7 PDE domain or N-terminally truncated AKAP7 (both lacking a nuclear localization motif), but not full-length AKAP7 or a mutant, AKAP7^{H185R}, PDE domain restored the infectivity of ns2 mutant MHV in bone marrow macrophages and in livers of infected mice. Interestingly, the AKAP7 PDE domain and N-terminally deleted AKAP7 were present in the cytoplasm (the site of MHV replication), whereas full-length AKAP7 was observed only in nuclei. We suggest the possibility that viral acquisition of the host AKAP7 PDE domain might have occurred during evolution, allowing diverse RNA viruses to antagonize the RNase L pathway.**

IMPORTANCE **Early virus-host interactions determine whether an infection is established, highlighting the need to understand fundamental mechanisms regulating viral pathogenesis. Recently, our laboratories reported a novel mode of regulation of the IFN antiviral response. We showed that the coronavirus MHV accessory protein ns2 antagonizes the type I IFN response, promoting viral replication and hepatitis. ns2 confers virulence by cleaving 2′,5′-oligoadenylate (2-5A) activators of RNase L in macrophages. We also reported that the rotavirus VP3 C-terminal domain (VP3-CTD) cleaves 2-5A and that it may rescue ns2 mutant MHV. Here we report that a cellular protein, AKAP7, has an analogous 2′,5′-phosphodiesterase (2′,5′-PDE) domain that is able to restore the growth of chimeric MHV expressing inactive ns2. The proviral effect requires cytoplasmic localization of the AKAP7 PDE domain. We speculate that AKAP7 is the ancestral precursor of viral proteins, such as ns2 and VP3, that degrade 2-5A to evade the antiviral activity of RNase L.**

Received 9 May 2014 **Accepted** 29 May 2014 **Published** 1 July 2014

Citation Gusho E, Zhang R, Jha BK, Thornbrough JM, Dong B, Gaughan C, Elliott R, Weiss SR, Silverman RH. 2014. Murine AKAP7 has a 2′,5′-phosphodiesterase domain that can complement an inactive murine coronavirus ns2 gene. mBio 5(4):e01312-14. doi:10.1128/mBio.01312-14.

Editor Herbert Virgin, Washington University School of Medicine

Address correspondence to Susan R. Weiss, weisssr@upenn.edu, or Robert H. Silverman, silverr@ccf.org.

This article is a direct contribution from a member of the American Academy of Microbiology.

Host antiviral pathways triggered by type I interferons (IFNs) are self-limiting so that after virus is eliminated, the host can restore normal cellular and tissue functions (1). Many types of viruses also prevent activation of host antiviral pathways (reviewed in reference 2). The 2′,5′-oligoadenylate (2-5A) synthetase (OAS)/RNase L system is one of the principal mediators of the IFN antiviral response (reviewed in references 3 to 6). Recently, we reported that two homologous viral proteins from unrelated viruses, coronavirus mouse hepatitis virus (MHV) strain A59 ns2 and group A rotavirus strain SA11 VP3, have 2′,5′-phosphodiesterase (2′,5′-PDE) activities that antagonize the antiviral activity of RNase L by degrading 2-5A [$p_x(5'A2'p)_n5'A$, where x is 1 to 3 and n is 2 or greater] (7, 8). ns2 and VP3 are eukaryotic-viral LigT-like family members that include both viral and cellular proteins of diverse origins, some of which possess cyclic nucleotide phosphodiesterase (CPD) activity (Fig. 1A) (9). LigT proteins are named for the prototypical archeo-bacterial tRNA-ligating enzyme LigT with reversible 2′-5′-RNA ligase activity (10) and are part of a larger superfamily of 2H phosphoesterases characterized by the presence of a pair of conserved His-h-Thr/Ser-h motifs (where h is typically a hydrophobic residue) (9, 11, 12). However, while MHV ns2 has 2′,5′-PDE activity, it apparently lacks CPD activity based on its inability to cleave 2′,3′ cyclic AMP (cAMP), 3′,5′ cAMP, and ADP-ribose 1″,2″ cyclic phosphate (7). Mutation of the active site of ns2 blocked MHV replication in liver, thereby preventing hepatitis in wild-type (wt)

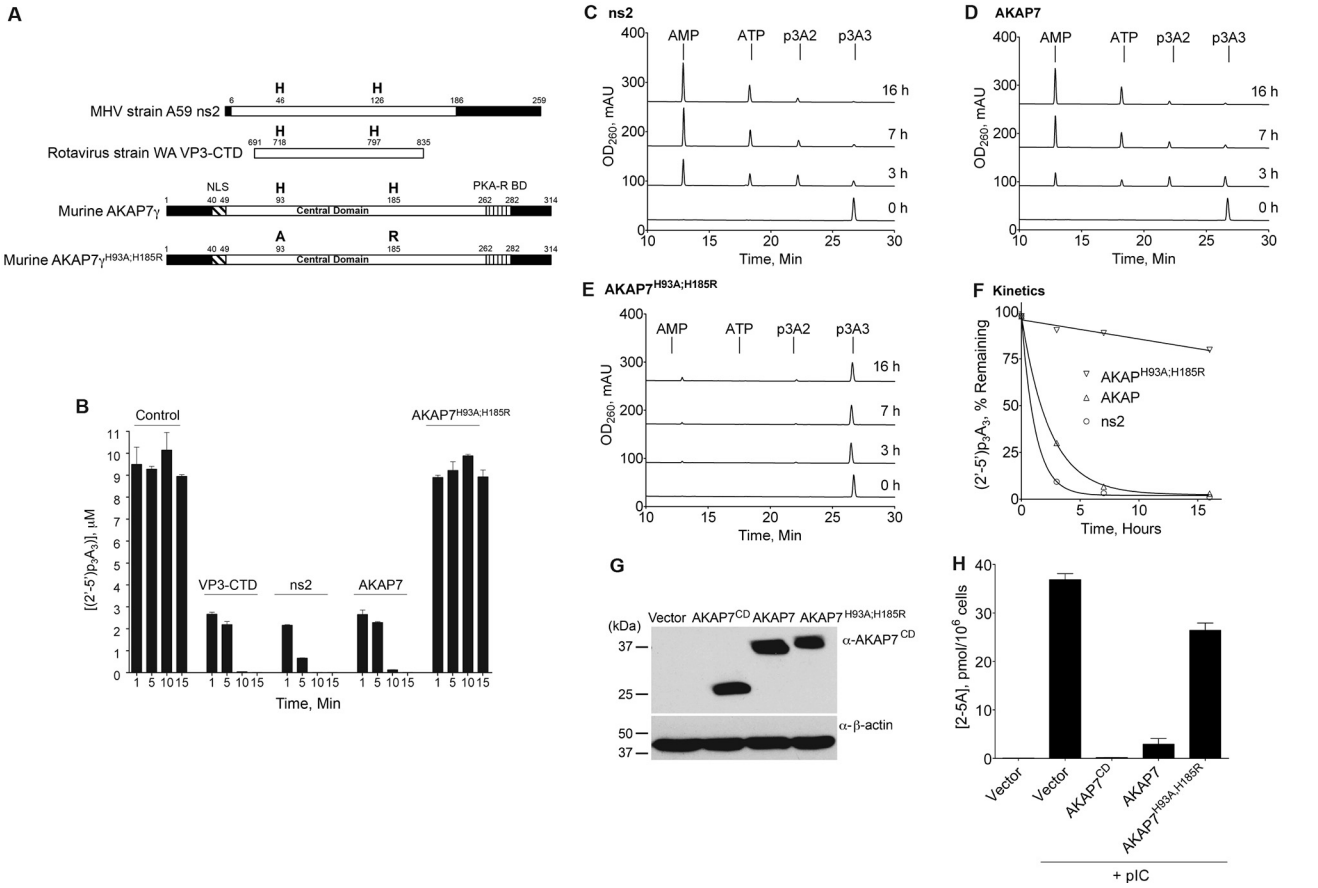

FIG 1 AKAP7 rapidly degrades 2-5A with kinetics similar to those of MHV strain A59 ns2 and human rotavirus strain WA VP3-CTD. (A) Diagrams of MHV strain A59 ns2, human rotavirus strain WA VP3-CTD, mouse AKAP7γ, and mutant AKAP7γ$^{H93A;H185R}$. NLS, nuclear localization signal; PKA-R BD, protein kinase A RI and RII subunit binding domain. Black regions represent undefined domains. (B) Degradation of (2′-5′)p_3A_3 *in vitro* at 37°C by the different purified proteins (indicated) as determined by FRET assays. Control, no protein added. Results are averages of values from three biological replicates, and the error bars are the standard deviations (SD). (C to E) Purified (2′-5′)p_3A_3 (10 μM) was incubated with 1.5 μM purified ns2, AKAP7, or AKAP7$^{H93A;H185R}$, respectively, at 22°C. At the times indicated (to the right), the reactions were stopped. The substrate, (2'-5')p_3A_3, and its degradation products (2′-5′)p_3A_2, 5′-AMP, and 5′-ATP (as indicated) were separated by HPLC. Elution times are shown on the *x* axes. OD_{260}, optical density at 260 nm; mAU, arbitrary units (in thousands). (F) The percentage of intact (2′-5′)p_3A_3 remaining was determined from areas under the peaks from chromatograms using 32 Karat software (Beckman Coulter, Inc.) and is plotted as a function of time. (G) Western blot analysis of AKAP7 proteins stably expressed in human Hey1B cells as determined by probing with a rabbit polyclonal antiserum against AKAP7 peptide B (see Materials and Methods). (H) Levels of 2-5A in Hey1B cells expressing different AKAP7 proteins (or vector control cells) transfected with pIC, as determined by FRET assays (see Materials and Methods). Results are averages from three biological replicates. Error bars represent SD.

mice but not in *RNasel*$^{-/-}$ mice (7). Furthermore, the group A rotavirus (strain SA11) VP3 C-terminal domain (CTD) was able to restore the replication and virulence of a chimeric ns2 mutant MHV in mice (8), showing that these two virally encoded activities are functionally equivalent. Homologous PDEs encoded by other 2a betacoronaviruses, toroviruses, and group A rotaviruses suggest that this is a general mechanism of host antagonism necessary for replication of many RNA viruses (5, 8, 9, 11; unpublished data).

A kinase anchoring proteins (AKAPs) are a family of scaffolding proteins that bind the regulatory (R) subunits of protein kinase A (PKA) to localize, coordinate, and regulate cAMP signaling during diverse processes, including cardiac excitation-contraction coupling, neuronal synaptic plasticity, sperm motility, insulin secretion, and renal homeostasis (reviewed in references 13 to 16). Muscle-specific AKAP (mAKAP) partners with a cAMP-specific phosphodiesterase, PDE4D3, which limits activation of PKA (17). Several other AKAPs also bind to different cyclic nucleotide PDEs (reviewed in reference 16). However, among more than 43 known AKAP family members (13), only long isoforms of AKAP7 (also known as AKAP15 or -18) have a central domain (CD) with two characteristic His-h-Thr/Ser-h motifs and predicted structural homology to the viral 2′,5′-PDEs MHV ns2 and rotavirus VP3 (Fig. 1A and see Fig. S1 in the supplemental material) (9, 12, 18). Therefore, we explored the possibility that instead of binding an extrinsic PDE like other AKAPs, AKAP7 might have an intrinsic PDE activity. There are four splice variants of AKAP7: (i) two short forms of 15 and 18 kDa (α and β) that have a membrane-targeting region and the PKA binding motif but lack the nuclear localization signal (NLS) and CD and (ii) two long forms of 37 and 42 kDa (γ and δ) that contain (from the N to the C terminus) an NLS, the CD, and the AKAP helix and leucine zipper that bind R subunits of PKA and also Ca^{2+} and Na^{+} channels (18). A recent report described a *cre/loxP* knockout in mice of AKAP7 exon 7

from all four AKAP7 splice variants (19). AKAP7 exon 7 encodes the C-terminally modified leucine zipper domain that binds the RI/RII PKA subunits, Ca^{2+} and Na^{+} channels, and the 3′ untranscribed region (3′-UTR). The AKAP7-deficient animals were, however, phenotypically normal. In particular, cardiomyocytes from AKAP7-deficient mice responded normally to adrenergic stimulation, leading the authors to suggest that another AKAP isoform performs this function (19). Here we investigated the possible role of AKAP7 in a biochemical function alternative to regulating cAMP signaling, namely, regulating 2-5A signaling to RNase L. We determined that the AKAP7 CD is a 2′,5′-PDE that rapidly degrades 2-5A. As a result, replication of an ns2 mutant MHV was restored by the AKAP7 CD or by an N-terminally truncated AKAP7 that retains the CD, both of which localized to the cytosol, the site of viral replication. However, full-length AKAP7 localized to the nucleus and failed to restore replication of ns2 mutant MHV. These studies identify a novel biochemical function of an AKAP family member and are consistent with the possibility that the AKAP7 CD has been acquired by some viruses to evade the antiviral activity of type I IFNs by preventing activation of RNase L (7, 8). In addition, our findings suggest that localization of 2-5A-degrading enzymes near sites of viral RNA synthesis may negate the antiviral activity of RNase L.

RESULTS

Murine AKAP7 rapidly degrades 2-5A with kinetics similar to those of MHV ns2 and rotavirus VP3. Alignment of murine AKAP7 to its eukaryotic homologs suggests that it is a member of an ancient family of 2H phosphoesterases that extend from plants to humans (Fig. S2). To determine whether murine AKAP7 is a 2′,5′-PDE, cDNA encoding full-length AKAP7γ (hereinafter "AKAP7" unless stated otherwise) was expressed in bacteria, purified, and tested for its ability to cleave the trimeric species of 2-5A, $(2'\text{-}5')p_3A_3$, *in vitro*. Wild-type (wt) AKAP7, AKAP7 mutated in both conserved histidines ($AKAP7^{H93A;H185R}$), and, for comparison, MHV strain A59 ns2 and human rotavirus strain WA VP3-CTD (Fig. 1A) were incubated with $(2'\text{-}5')p_3A_3$ at 37°C. 2-5A levels were measured by activation of RNase L *in vitro* in comparison to a standard curve of 2-5A dilutions using a previously described fluorescence resonance energy transfer (FRET) method (20). ns2, VP3, and AKAP7 (each at 1.5 μM) rapidly degraded $(2'\text{-}5')p_3A_3$ (10 μM) such that after a 1-min incubation at 37°C, less than 30% of the input $(2'\text{-}5')p_3A_3$ remained intact (Fig. 1B). Little or no detectable 2-5A remained after 10 min of incubation with any of the three proteins. In contrast, AKAP7 mutated in the two conserved histidine residues lacked the ability to degrade 2-5A (Fig. 1B).

To demonstrate that AKAP7 has a 2′,5′-PDE activity that cleaves one 5′-AMP at a time from the 2′,3′ terminus of 2-5A, we performed incubations at a lower temperature, 22°C. As we reported previously (7), ns2 degrades $(2'\text{-}5')p_3A_3$ to $(2'\text{-}5')p_3A_2$ and 5′-AMP, and then the diadenylate $(2'\text{-}5')p_3A_2$ is degraded to 5′-AMP and 5′-ATP (Fig. 1C). AKAP7 also removed one 5′-AMP at a time from trimeric 2-5A, and therefore it is also a bona fide 2′,5′-PDE (Fig. 1D). As expected, active-site mutant $AKAP7^{H93A;H185R}$ failed to degrade $(2'\text{-}5')p_3A_3$ (Fig. 1E). Quantitation of these results showed that AKAP7 and ns2 displayed comparable kinetics (Fig. 1F).

AKAP7 degrades 2-5A in intact cells transfected with dsRNA. To determine if AKAP7 was able to degrade 2-5A in intact cells, cDNAs for full-length AKAP7, AKAP7 CD, and mutant $AKAP7^{H93A;H185R}$ (with a C-terminal Flag epitope) were transiently expressed in the human ovarian carcinoma cell line Hey1B (21). Hey1B cells were selected for these experiments because endogenous AKAP7 was undetectable by Western blotting with a rabbit polyclonal antibody against an AKAP7 CD peptide (Fig. 1G). Ectopic expression of the different AKAP7 proteins was confirmed by immunoblotting (Fig. 1G). At 20 h posttransfection with either an empty vector or the AKAP7 cDNAs, cells were transfected for an additional 3 h with the synthetic double-stranded RNA (dsRNA) poly(rI) · poly(rC) (pIC), a potent activator of OAS (22). 2-5A was undetectable in control cells transfected with the vector alone as determined by FRET (the lower limit of detection was about 15 fmol/10^6 cells) (Fig. 1H). However, pIC caused high levels of 2-5A (38 pmol/10^6 cells) to accumulate in the vector control cells. In contrast, expression of the AKAP7 CD reduced pIC induction of 2-5A by almost 200-fold (to 0.2 pmol/10^6 cells). The full-length AKAP7 reduced pIC-induced levels of 2-5A by about 12-fold (to 3 pmol/10^6 cells), while full-length mutant $AKAP7^{H93A;H185R}$ failed to deplete pIC-induced levels of 2-5A (26 pmol/10^6 cells remaining). These findings demonstrate that AKAP7 (full length and CD) effectively degraded 2-5A in intact pIC-transfected cells.

Viral expression of AKAP7 in BMM. To determine if AKAP7 could functionally replace ns2, we further exploited an MHV-A59 reverse-genetics system (7, 8, 23). We hypothesized that the expression of AKAP7 from a chimeric ns2 mutant MHV would restore viral replication in B6 bone marrow-derived macrophages (BMM). Four MHV-AKAP7 chimeric viruses, all based on the $ns2^{H126R}$ mutant MHV, were constructed (Fig. 2A) by inserting coding sequences for full-length AKAP7 ($ns2^{H126R}$-AKAP7), AKAP7 with an N-terminal domain (NTD) truncation ($ns2^{H126R}$-$AKAP7^{\Delta NTD}$), the AKAP7 CD ($ns2^{H126R}$-$AKAP7^{CD}$), or a mutant AKAP7 CD ($ns2^{H126R}$-$AKAP7^{CD\ H185R}$) into the MHV nonessential ns4 gene (Fig. 2A). BMM (*Rnasel*$^{-/-}$) were infected with each chimeric virus, as well as with control wt A59 and $ns2^{H126R}$, for 10 h at a multiplicity of infection (MOI) of 1. All viruses expressed similar levels of ns2 and AKAP7 proteins of the expected sizes in infected BMM as determined by Western blotting (Fig. 2B).

Intracellular localization of wt and mutant AKAP7 proteins. Full-length AKAP7 has an NLS sequence at its N terminus which was deleted from the other AKAP7 constructs (Fig. 1A and 2A). We compared the subcellular localizations of the AKAP7 proteins expressed by each of the chimeric viruses. Indirect immunofluorescence analysis with antibody against an AKAP7 CD peptide was carried out in 17CL-1 fibroblasts and BMM, neither of which expresses a detectable level of endogenous AKAP7. Full-length AKAP7 was located in the nuclei of both 17Cl-1 and B6 BMM, as was previously reported (Fig. 3A and B) (24). The N-terminal deletion (ΔNTD) including the NLS caused the truncated AKAP7 protein to localize exclusively to the cytoplasm of 17Cl-1 cells but to both the nuclei and the cytoplasm of BMM (Fig. 3A and B and data not shown). The CD of AKAP7 and its mutant (also missing the NLS) localized to the cytoplasm of 17Cl-1 cells but, like $AKAP7^{\Delta NTD}$, localized to both the cytoplasm and the nuclei of BMM. Likewise, the ns2 protein was clearly cytoplasmic in 17Cl-1 cells but present in both the nuclei and the cytoplasm of BMM. To confirm these findings, human 293T cells were stably transfected with cDNA expressing full-length AKAP7, the AKAP7 CD, or, as a control, the empty vector. Western blots showed that the 293T cells also failed to express detectable levels of endogenous AKAP7,

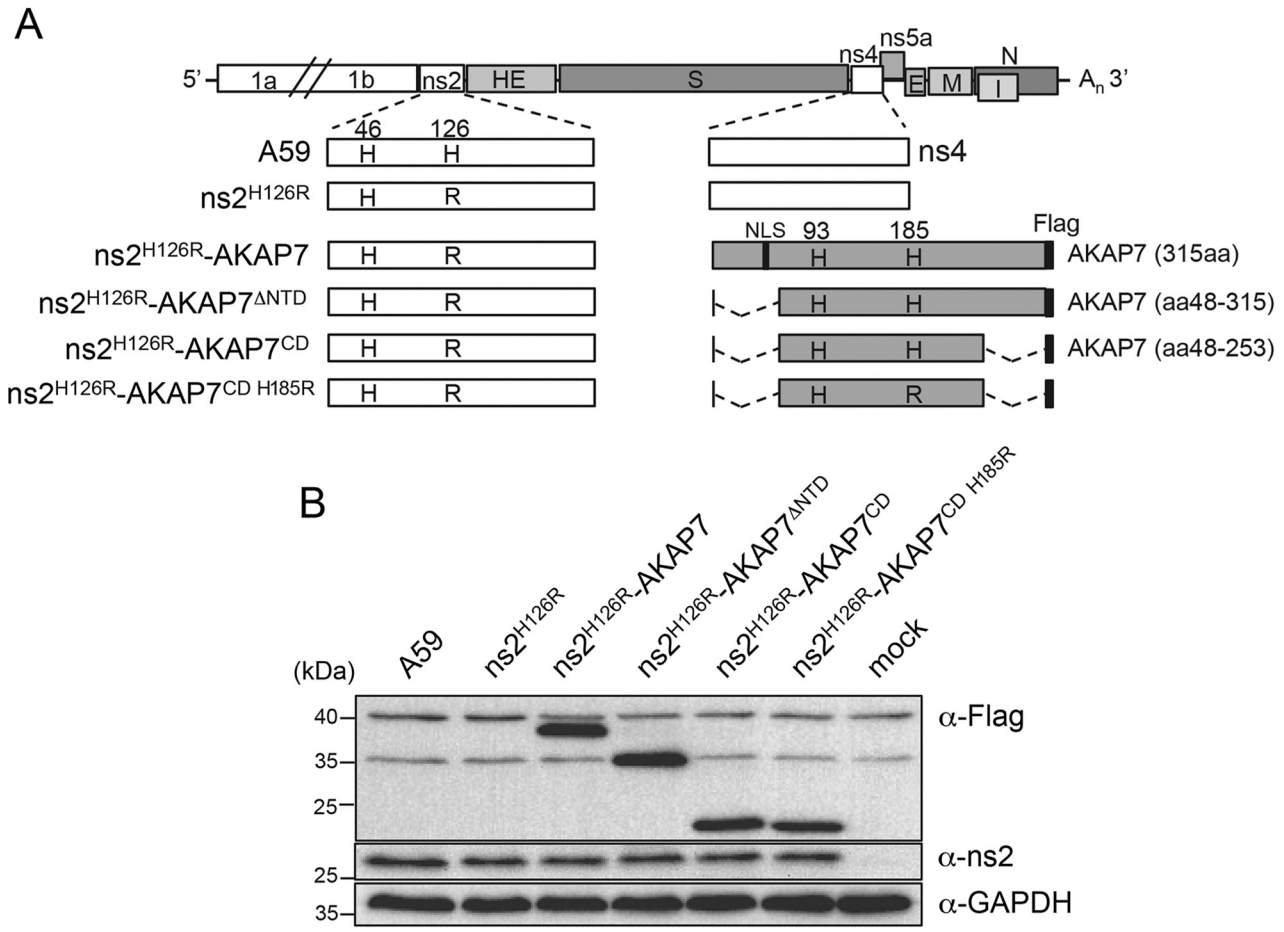

FIG 2 Construction of chimeric viruses expressing AKAP7 proteins. (A) Schematic diagram of the mutant ns2 and chimeric AKAP7 viruses. The AKAP7 cDNAs for Flag-tagged full-length and N-terminally truncated CD and its histidine mutant were inserted in place of *ns4*. The numbers above the boxes indicate the locations of histidine residues critical for the function of ns2 or AKAP7 protein (histidine-to-arginine mutations are shown in the boxes). The location of the predicted NLS is also indicated. aa, amino acids. (B) Verification of the expression of MHV ns2 proteins and AKAP7 proteins. *Rnasel*$^{-/-}$ BMM were infected (1 PFU/cell) for about 10 h, and total cellular proteins were harvested and subjected to SDS-PAGE and Western blot analysis. Cellular GAPDH was monitored as a loading and transfer control.

whereas both AKAP7 and AKAP7 CD were clearly present in the transfected cells (Fig. 3C). As expected, full-length AKAP7 localized to the nuclei, whereas AKAP7 CD, which lacks the NLS, localized to the cytoplasm (Fig. 3D). These studies show that expressed full-length AKAP7 is nuclear but that deletion of its NLS causes some or all of the truncated protein to localize to the cytoplasm, depending on the cell type.

AKAP7 polypeptides that localize to the cytoplasm restore the replicative capacity of ns2 mutant MHV in BMM of wt B6 mice. To determine the effect of AKAP7 on viral replication, BMM from wt B6 or *Rnasel*$^{-/-}$ mice were infected with AKAP7 chimeric viruses or with control wt A59 and mutant $ns2^{H126R}$. As expected, the replication of $ns2^{H126R}$ was severely impaired (by 3 $\log_{10}$ units) compared to that of wt A59 in B6 BMM (Fig. 4A), consistent with the results of our previous studies (7, 8, 25). Intriguingly, chimeric $ns2^{H126R}$-AKAP7 was unable to rescue replication in B6 BMM, demonstrating that the expression of full-length AKAP7 does not confer a wild-type level of replication in B6 BMM. In contrast, viruses expressing either the N-terminally deleted AKAP7 ($ns2^{H126R}$-$AKAP7^{\Delta NTD}$) or AKAP7 CD ($ns2^{H126R}$-$AKAP7^{CD}$) replicated to levels similar to those of wt A59, showing that either of these truncated forms of AKAP7 can compensate for the inactive $ns2^{H126R}$ PDE. However, when catalytic histidine residue 185 in the AKAP7 CD was mutated, replication of the chimeric $ns2^{H126R}$-$AKAP7^{CD\ H185R}$ virus was impaired to an extent similar to that with the $ns2^{H126R}$ mutant. As expected, however, all of these chimeric viruses replicated efficiently, to an extent and with kinetics similar to those of wt A59 in BMM derived from *Rnasel*$^{-/-}$ mice (Fig. 4B). These results show that expression of the N-terminal truncation or of the CD of AKAP7, both of which lack the NLS and are present in the cytoplasm, can restore the function of ns2 in the mutant virus, whereas full-length AKAP7, which localizes to the nuclei, cannot. In addition, the ability of the AKAP7 CD to rescue ns2 mutant MHV is dependent on a catalytic histidine residue.

Expression of the N-terminally deleted AKAP7 or the CD of AKAP7 inhibits RNase L-mediated rRNA degradation induced by the ns2 mutant virus in B6 BMM. To further investigate whether the restoration of ns2 mutant virus replication by AKAP7 CD or N-terminally deleted AKAP7 expression is due to antagonism

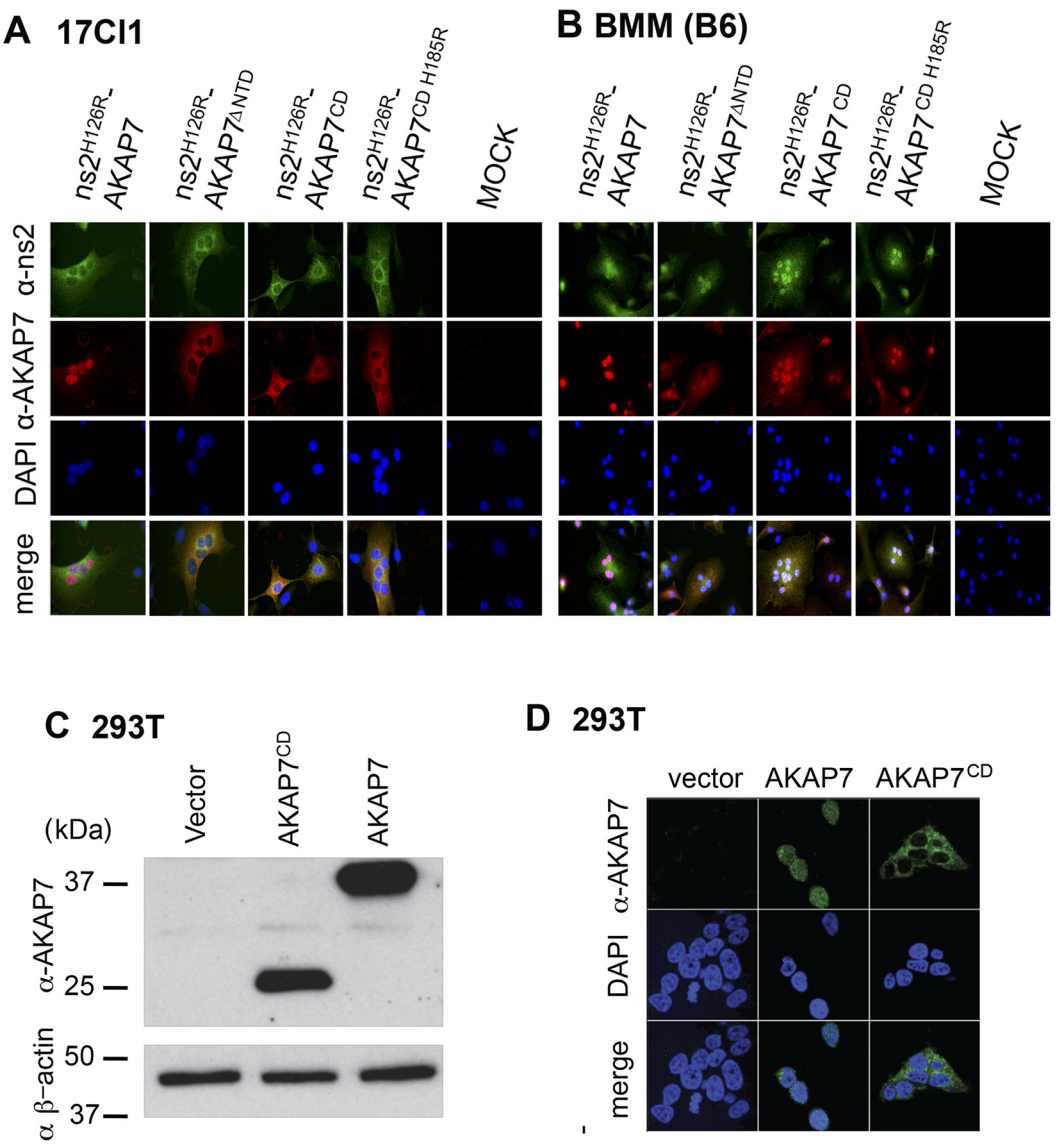

FIG 3 Cellular localization of the AKAP7s in different cell types. 17Cl-1 cells (A) and B6 BMM (B) were infected with chimeric MHV viruses expressing full-length AKAP7, N-terminally truncated AKAP7 ($AKAP7^{\Delta NTD}$), the CD of AKAP7 ($AKAP7^{CD}$), or its mutant ($AKAP7^{CD\ H185R}$) and stained for the expression of ns2 and AKAP7 with monoclonal antibodies against ns2 or against murine AKAP7 CD peptide A. DAPI was used to visualize nuclei. Magnification for panels A and B, ×60. (C) 293T cells expressed AKAP7 or $AKAP^{CD}$ from lentivirus vectors (indicated). Western blot detection of AKAP7 and the AKAP7 CD by immunoblotting with anti-AKAP7 CD antibody (peptide B) and with antibody against β-actin as a loading and transfer control is shown. (D) 293T cell lines expressing AKAP7 or the AKAP7 CD (as in panel C) were stained with a polyclonal antiserum against murine AKAP7 CD peptide A. Nuclei were visualized with DAPI staining. Magnification, ×63.

of RNase L activity, we analyzed the integrity of rRNA in BMM infected with each recombinant virus. RNase L cleaves rRNA in intact ribosomes, resulting in a characteristic set of discrete rRNA cleavage products (26, 27). BMM infected with each virus were lysed at 10 h postinfection, and RNA was extracted and analyzed with an RNA chip (see Materials and Methods) (28). The chimeric viruses expressing either the AKAP7 N-terminally truncated protein or the CD prevented rRNA degradation by RNase L, as with wt A59, while cells infected with the chimeras expressing full-length AKAP7 degraded RNA to an extent similar to that of the $ns2^{H126R}$ mutant or the double mutant $ns2^{H126R}$-$AKAP7^{CD\ H185R}$ (Fig. 4C). These findings show that an AKAP7 polypeptide containing the PDE domain but lacking the NLS prevents activation of RNase L in the cytoplasm, whereas full-length AKAP7, which localizes to the nucleus, or mutant AKAP7 CD does not.

Expression of the AKAP7 CD enhances replication of ns2 mutant virus in liver. We have previously shown that the ns2 mutant is highly attenuated for replication and pathogenesis in the livers of B6 mice, but it replicated and induced hepatitis to an extent similar to that of wt A59 in *Rnasel*$^{-/-}$ mice (7, 12, 25). To determine if expression of AKAP7 is able to compensate for an inactive ns2 protein and confer liver replication *in vivo*, B6 and *Rnasel*$^{-/-}$ mice were infected intrahepatically with viruses expressing the AKAP7 CD or its mutant as well as A59 and $ns2^{H126R}$.

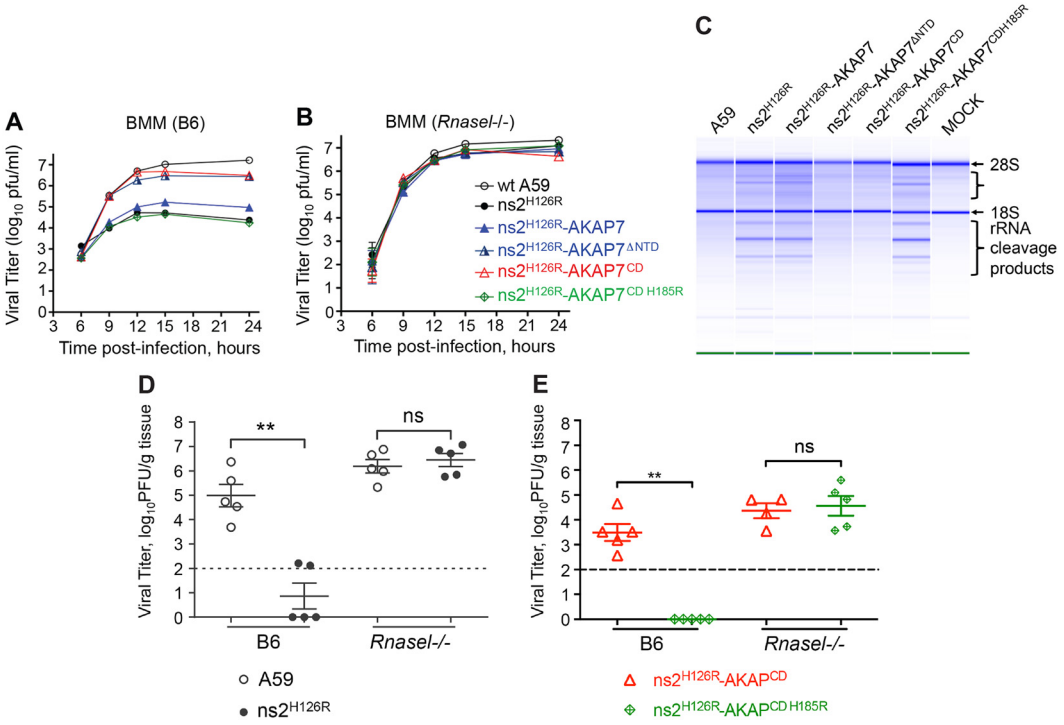

FIG 4 Expression of the N-terminal truncation or the CD of AKAP7 restores the replication of mutant ns2 *in vitro* and *in vivo*. Growth kinetics of chimeric AKAP7 viruses were determined on BMM from B6 mice (A) and *Rnasel*$^{-/-}$ mice (B). BMM were infected with each virus (as indicated) at an MOI of 1. Samples of the cultured supernatant were taken at the indicated time points, and viral titers were determined by plaque assays. The data are from one representative experiment of at least two, each performed in triplicate. (C) AKAP7 CD and N-terminally truncated proteins inhibit rRNA degradation during viral infection. B6 BMM were infected (MOI of 1) and harvested at 10 h postinfection, and the integrity of total cellular RNA was analyzed on RNA chips (Agilent). (D and E) Four-week-old B6 or *Rnasel*$^{-/-}$ mice were infected with 2,000 PFU/mouse intrahepatically with A59 and ns2^{H126R} (D) or ns2^{H126R} AKAP7^{CD} and the double mutant ns2^{H126R} AKAP7$^{CD\ H185R}$ (E). At day 5 postinfection, mice were sacrificed, and viral titers in the liver were determined by plaque assays. The dashed line represents the limit of detection, and error bars represent standard errors of means ($n = 5$). Asterisks indicate that differences are statistically significant (**, $P < 0.05$). Data are derived from one representative experiment of two. ns, not statistically significant.

The virus titers in liver were determined at day 5 postinfection, the peak day for viral replication in this organ. As expected, ns2^{H126R} virus replicated minimally in B6 mice but recovered to wt A59 virus replication levels in *Rnasel*$^{-/-}$ mice (Fig. 4D). The chimeric ns2^{H126R}-AKAP7^{CD} virus replicated in B6 mice to a titer of 10^4 PFU/g tissue, while the isogenic AKAP7 mutant ns2^{H126R}-AKAP7$^{CD\ H185R}$ virus failed to replicate above the level of detection ($P < 0.001$) (Fig. 4E). Both of the chimeric AKAP7 viruses replicated equally in *Rnasel*$^{-/-}$ mice to a level similar to that of the ns2^{H126R}-AKAP7^{CD} virus in B6 mice. These results suggested that expression of the active AKAP7 CD promotes the replication of ns2 mutant virus in livers of wt B6 mice. Furthermore, virus replication in the liver required the active-site residue, histidine-185. Taken together, our findings suggest that the AKAP7 CD can restore the replication of mutant ns2 virus *in vivo* as a result of its 2′,5′-PDE activity, which cleaves 2-5A and thereby prevents RNase L activation in the cytoplasm.

DISCUSSION

Control of viral infections by regulation of 2-5A turnover. Our findings establish the AKAP7 CD as a 2′,5′-PDE that is able to substitute for a viral enzyme, MHV ns2, with the same activity. 2′,5′-PDEs that cleave 2-5A to ATP and AMP and phosphatases that remove the 5′-terminal phosphates on 2-5A prevent perpetual activation of RNase L after the viral infection is cleared and thereby limit RNA damage to the host (29, 30) (reviewed in reference 5). *In vitro*, enzymes with 5′-phosphatase activity, such as alkaline phosphatase, can remove the 5′-triphosphate moiety of 2-5A, thus eliminating, or greatly reducing, the ability of the core 2′,5′-oligoadenylate to activate RNase L (31). In addition, porcine coronavirus transmissible gastroenteritis virus (TGEV) gene 7 protein has been reported to dephosphorylate 2-5A through its interactions with protein phosphatase PP1 (32). Two mammalian PDEs, PDE12 (2′-PDE) (33–35) in the exonuclease-endonuclease-phosphatase family of deadenylases and ectonucleotide pyrophosphatase/phosphodiesterase 1 (ENPP1) (36), have been shown to degrade 2-5A *in vitro*. PDE12 is a mitochondrial protein with both 2′,5′- and 3′,5′-PDE activities that removes poly(A) tails from mitochondrial mRNAs (34, 35). ENPP1 has a catalytic domain that is extracellular and is therefore essentially an extracellular enzyme; in addition to degrading 2-5A, it cleaves phosphodiester bonds in 3′,5′ RNA, DNA, and cAMP (36). In contrast to PDE12 and ENPP1, which have mitochondrial and extracellular locations, respectively, OAS proteins localize to either the cytoplasm or nuclei, also sites of virus replication (37, 38). Our findings here demonstrate that AKAP7 is an additional host enzyme with 2′,5′-PDE activity. Among the host 2′,5′-PDEs described to date, only AKAP7 is a 2H-phosphoesterase family member with homology to the viral enzymes of the same class.

A prior study with a commercial AKAP7 antibody (from Pro-

teintech) showed widespread expression of AKAP7 in different mouse organs, including heart, brain, skeletal muscle, kidney, and lung (19). Using the same antibody, we were able to detect low levels of AKAP7 in Hey1b cells and BMM. However, AKAP7 mRNA is not induced by wt A59 or ns2 mutant infection (unpublished data). Thus, AKAP7 may be functional at a low expression level, may be expressed at higher levels in some tissues (presently under investigation), and/or may be induced by cytokines or other soluble mediators not induced by MHV.

Cytoplasmic expression of the AKAP7 PDE rescues ns2 mutant MHV. AKAP7 is one of a relatively few members of the AKAP family that localizes to the nucleus (24, 39). Although expressed full-length AKAP7 traffics to nuclei, the AKAP7 central PDE domain typically localizes to the cytoplasm, or to both the cytoplasm and nuclei, after the N-terminal NLS is deleted (Fig. 3) (24). 2-5A produced in the cytoplasm during viral infections might be expected to transit nuclear pores, leading to its degradation by endogenous nuclear AKAP7. However, expression of full-length AKAP7 failed to rescue ns2 mutant MHV or to prevent RNase L activation in the infected wt BMM. In contrast, the AKAP7 CD rapidly degraded 2-5A, preventing activation of RNase L and restoring the ability of an ns2 mutant MHV to replicate *in vitro* and *in vivo*. MHV RNA replication occurs completely in the cytoplasm of transformed cell lines (40), and the local requirement for degradation of 2-5A may not be so surprising. Nilsen and Baglioni (41) proposed, based in part on their experiments with encephalomyocarditis virus, that microdomains (localized accumulations) of 2-5A occur at the sites of viral double-stranded replication intermediates (RI), where OAS binds and is activated, causing localized activation of RNase L. Thus, 2′,5′-PDE activity may be required in the same subcellular compartment as viral RNA replication to effectively antagonize RNase L activation, as measured by virus rescue as well as protection of rRNA. These findings raise the possibility of an additional, yet-to-be identified isoform of AKAP7 that retains the CD but localizes to the cytoplasm. Alternatively, AKAP7 may be relevant to viruses that replicate in nuclei but not to viruses, such as coronaviruses or rotaviruses, that replicate in the cytoplasm. It remains to be determined, however, whether the endogenous, nuclear AKAP7 has any role in viral infections. Alternatively, it is also possible that AKAP7 functions to degrade nuclear 2-5A or 2-5A-like molecules that might be produced during nonviral cellular responses to stress (42). However, full-length AKAP7 was able to degrade 2-5A in cells transfected with pIC, although less effectively than the AKAP7 CD, perhaps due to some leakage of the overexpressed AKAP7 into the cytoplasm (Fig. 1H). Moreover, the intracellular localizations of transfected pIC and the MHV RI are likely to be different. In addition, posttranslational modifications, such as phosphorylation, may cause AKAP7 to relocate to different intracellular sites, as suggested for the AKAP species Chd8 (39).

The titers of ns2 mutant chimeric viruses with AKAP7 genes inserted in the place of MHV gene 4 are all significantly lower than those with the natural gene 4 sequences (Fig. 4D and E). This is similar to our findings with VP3-CTD/MHV chimeric viruses, which reached liver titers similar to those of the AKAP7-CD chimeras (8). The reduction in viral titers is most likely due to attenuation associated with disturbing the genome in the region of gene 4, which is not required for viral replication or virulence (43). This explanation is supported by our finding that a virus expressing wt ns2 and mutant VP3-CTD from the gene 4 position is as attenuated as virus expressing mutant ns2 and wt VP3-CTD from the gene 4 position (data not shown). Because the replication of these chimeric viruses in the liver is so much less robust than that of wt A59, it was not possible to determine whether expression of foreign PDEs fully confers hepatitis on the ns2^{H126R} mutant.

Coronavirus replication is reported to occur only in the cytoplasm of infected cells (40) and to involve the rearrangement of cellular membranes into double-membrane vesicles and convoluted membranes, the sites of viral RNA replication (44, 45). As expected, in infected murine fibroblasts, coronavirus proteins are localized in the cytoplasm, as shown in Fig. 3A. Most, if not all, studies of localization of MHV-encoded proteins or membrane rearrangement have been carried out with transformed cell lines, and there is little information on infection of primary cells such as BMM. Interestingly, full-length AKAP7 retains its exclusively nuclear localization in BMM, whereas the N-terminally deleted AKAP7 and AKAP7 CD as well as ns2 were present in both the cytoplasm and the nucleus (Fig. 3B). Future studies will be directed at comparing the subcellular localization of proteins and replication complexes in MHV-infected primary cells to those in transformed cell lines. Nevertheless, rescue of the ns2 mutant phenotype occurs only when at least some of the AKAP PDE is localized to the cytoplasm.

Relationship between viral and cellular eukaryotic-viral LigT-like members of the 2H phosphoesterase superfamily. Degradation of 2-5A appears to be a general strategy of many RNA viruses for preventing activation of RNase L, which would otherwise block viral replication. Group 2a betacoronaviruses, which have plus-strand RNA genomes, and the group A rotaviruses, with segmented dsRNA genomes, are unrelated RNA viruses with different replication strategies, yet both encode related 2′,5′-PDEs, ns2 and VP3, respectively (7, 8). Here we present the first evidence that a viral pathogen for humans, the rotavirus strain WA (46), also encodes a functional 2′,5′-PDE (Fig. 1B). In addition, many related viruses encode predicted or confirmed 2′,5′-PDEs, including additional 2a betacoronaviruses, human OC43 and HEC4408, bovine coronavirus, porcine hemagglutinating virus, the torovirus and coronavirus superfamily member equine torovirus (Berne), and group A, B, and G rotaviruses (reviewed in reference 5). While the evolutionary origins of these viral 2′,5′-PDEs are unknown, we suggest that the host AKAP7 2′,5′-PDE domain coding sequence might have been captured through RNA recombination during viral infections in the distant past. Alternatively, the viral PDEs may have evolved from other vertebrate 2H phosphoesterases (9). The phylogenetic relationship of different species of AKAP7, VP3 and ns2, based on protein sequence data was explored by means of fast minimum evolution (see Fig. S3 in the supplemental material). While this analysis shows a close relationship among different species of AKAP7, VP3, pp1a, and ns2, it does not reveal whether this relationship is the result of divergent or convergent evolution (Fig. S3). Coronavirus mRNAs are transcribed from their genomes by a discontinuous process believed to involve switching of template by the viral replicase complex. During this process, there is a high rate of homologous recombination, reportedly up to 25%, observed during *in vitro* replication and *in vivo* (reviewed in reference 47); this high-frequency template switching may result in low-frequency copying of host mRNA. Indeed, sequences homologous to the 5′ end of major histocompatibility complex (MHC) class I coding regions are found on the 5′ end of the MHV HE gene, adjacent to the 3′ end of the ns2 open

reading frame, and it was previously speculated that this was a result of homologous recombination between the MHV genome and host RNA (48). We suggest that AKAP7 PDE sequences have been acquired by a similar process and subsequently evolved into ns2. In support of this idea, an alignment of the amino acid sequences of different isoforms of AKAP7, ns2 and VP3, show extensive homology that extends beyond the His-h-Thr/Ser-h motifs (Fig. S1). Subsequent to randomly acquiring the AKAP7 CD coding sequence, the virus would have a selective advantage resulting in retention of the gene.

MATERIALS AND METHODS

Cell lines and mice. Murine 17Cl-1, L2 fibroblast, and BHK MHV receptor (MHVR) cells were cultured as described previously (12, 23). Human 293T (ATCC) and human Hey1B (21) cells were cultured in Dulbecco's modified Eagle's medium (DMEM) and RPMI 1640, respectively, both with 10% fetal bovine serum (FBS). Primary BMM were generated from the hind limbs of C57BL/6 (B6) or *Rnasel*$^{-/-}$ mice and cultured as described previously (49). C57BL/6 (B6) mice were purchased from the Jackson Laboratory. *Rnasel*$^{-/-}$ mice (B6, 10 generations of backcrossing) (50, 51) were bred in the University of Pennsylvania animal facility under an approved IACUC protocol.

Antibodies. The following antibodies were used: mouse anti-ns2 monoclonal antibody (provided by Stuart Siddell, University of Bristol, United Kingdom), mouse monoclonal anti-Flag epitope (M2; Sigma); sheep anti-mouse IgG and horseradish peroxidase (HRP)-linked whole antibody (GE Healthcare); horse anti-mouse IgG HRP-linked antibody, goat anti-rabbit IgG HRP-linked antibody (Cell Signaling); Alexa Fluor 488 goat anti-mouse IgG, Alexa Fluor 594 goat anti-rabbit IgG secondary antibodies, and Alexa Fluor 488 goat anti-rabbit IgG (Invitrogen); mouse anti-glyceraldehyde 3-phosphate dehydrogenase (GAPDH) (U.S. Biologicals); monoclonal anti-β-actin (A1978; Sigma-Aldrich); and custom-made affinity-purified rabbit polyclonal anti-AKAP7^{CD} antibodies against peptide A (CQLLNEDEVNIGTDALLELK) and peptide B (KKQSNGYYHCESSIVIGEK) (Biosynthesis). Peptide A is 100% homologous to murine AKAP7 (except in the N-terminal cysteine residue), whereas peptide B is 100% homologous to both mouse and human AKAP7.

Plasmids. For protein purification, the murine AKAP7 full-length coding sequence (clone MmCD00295344 from the PlasmID DF/HCC Resource Core at Harvard University [NCBI reference sequence NP_061217.3]) was transferred from the entry vector pENTR223.1 to a destination vector, pDest-pGEX-6P-1, using Gateway cloning technology (Life Technologies), resulting in pGEX-AKAP7. The histidine residues at positions 93 and 185 were mutated with a QuikChange II XL site-directed mutagenesis kit (Agilent) to generate pGEX-AKAP7 (H93A H185R). Plasmid pMAL-ns2 was described previously (7). The cDNA encoding the C-terminal domain (CTD) of human rotavirus WA strain VP3 (amino acids 691 to 835) (Virus Sequence Database accession number JX406749) was optimized for bacterial expression, synthetically made (GenScript, Piscataway, NJ), cloned in a pMal parallel vector, and expressed as a maltose binding protein fusion protein with a TEV cleavable tag, as we previously described for SA11 VP3-CTD (8). For Hey1b transient transfections, the murine AKAP7 full-length coding sequence was PCR amplified from the entry vector pENTR223.1 and cloned into the mammalian expression vector pCAGGS, generating pC-AKAP7. The histidine residues at positions 93 and 185 were mutated to generate pC-AKAP7(H93A; H185R), and a Flag tag sequence for the C terminus was added. The CD region of murine AKAP7 (corresponding to amino acids 48 to 253) was PCR amplified from the full-length construct with a Flag epitope sequence added to the C terminus and cloned into pCAGGS, generating pC-AKAP7 CD. For 293T stable cells lines, the lentivirus vector pLentiCMV-Puro-DEST, from Eric Campeau (52), pCMV-VSV-G, expressing vesicular stomatitis virus G envelope protein, and the pCMV-dR8.2 packaging plasmid, from Robert Weinberg (53), were obtained from Addgene. The murine AKAP7 full-length cDNA insert was transferred from the entry vector pENTR223.1 into the destination vector pLentiCMV-Puro-DEST with Gateway cloning technology. The CD region of murine AKAP7 (see above) was PCR amplified from the full-length construct with a Flag epitope sequence added to the C terminus and cloned into the entry vector pENTR2B (Gateway; Life Technologies). The insert was transferred to the destination vector pLentiCMV-Puro-DEST with Gateway technology. All of the clones were verified by nucleotide sequencing.

Viruses. Wild-type A59 and mutant ns2^{H126R} virus were described previously (8). The chimeric AKAP7 viruses were constructed based on the infectious cDNA clone icMHV-A59 (provided by Ralph S. Baric, University of North Carolina at Chapel Hill) (8, 23). All chimeric AKAP viruses encode the mutant ns2^{H126R} gene. To insert the AKAP7 sequences in place of *ns4*, the BsmBI restriction site in the AKAP7 gene was first removed by PCR-based site-directed mutagenesis with no change in coding sequence. The full-length AKAP7 (encoding 314 amino acids), AKAP7 with an N-terminal 47-amino-acid deletion (AKAP7$^{\Delta NTD}$, amino acids 48 to 314), and the CD of AKAP7 (AKAP7^{CD}, amino acids 48 to 253) were amplified and digested with SalI and NotI and cloned into icMHV-A59 fragment G as previously described for VP3-CTD (8). In the mutant AKAP$^{CD\ H185}$, the histidine at position 185 was exchanged for arginine (H185R, CAC to CGC), and the mutant sequence was cloned into icMHV-A59 fragment G using the same strategy as for the wild-type genes. All clones were confirmed by DNA sequencing.

The full-length A59 genome cDNA was assembled, and the recombinant viruses were recovered as previously described (8, 23, 54). Briefly, wild-type A-E plasmids, F plasmid with a single mutation (H126R) in ns2 (8), and G plasmids with AKAP7 insertions were digested with appropriate restriction enzymes, and the viral genome fragments were assembled *in vitro* to produce a full-length-genome infectious DNA. Viral RNA transcripts were generated from the DNA by using the mMessage mMachine T7 transcription kit (Ambion). The viral genome transcripts combined with the *in vitro* transcripts of viral nucleocapsid gene were electroporated into the BHK MHVR cells with a Bio-Rad Gene Pulser II electroporator. When virus cytopathology was observed, cell lysates were combined with the supernatant, virus plaque purified, and amplified on 17Cl-1 cells for use.

2′,5′-PDE activity assays. Proteins were expressed from the pGEX or pMAL construct in the BL21(DE3)/pLysS strain of *Escherichia coli* (Life Technologies). Wild-type or mutant AKAP7 was cleaved from the glutathione *S*-transferase (GST) fusion proteins bound to glutathione-Sepharose beads with 30 units of human rhinovirus HRV3C protease (PreScission protease; GE Healthcare). The cleaved proteins were analyzed by SDS-PAGE and staining with GelCode blue stain reagent (Thermo Scientific). The proteins were further purified by ion-exchange chromatography using a MonoQ GL100 column on an ÄKTApurifier UPC (GE Healthcare Life Sciences). The buffer in the pooled fractions was exchanged with assay buffer (20 mM HEPES, pH 7.2, 10 mM $MgCl_2$, and 1 mM dithiothreitol [DTT]) in Centriprep centrifugal filter devices (Millipore; molecular weight cutoff, 3 kDa). MHV ns2 was expressed in bacteria and purified as described previously (7). The plasmid encoding WA VP3-CTD was expressed in bacteria, and the WA VP3-CTD was purified essentially as described previously for SA11 VP3-CTD (8). Purified proteins (1.5 μM ns2, VP3, AKAP7, AKAP7$^{H93A;H185R}$) were incubated with 10 μM (2′-5′)p_3A_3 as described previously (7) in assay buffer at 22°C or 37°C. Degradation of the (2′-5′)p_3A_3 was determined by FRET-based RNase L activity assays, in comparison to a standard curve with different concentrations of (2′-5′)p_3A_3 (20), or with high-performance liquid chromatography (HPLC) as we described previously (55).

Degradation of 2-5A in pIC-transfected cells. Hey1B cells were plated at 4×10^5 cells/well in six-well plates for 20 h. Plasmid DNAs (1 μg per well) of the empty vector (pCAGGS), AKAP7^{CD}, AKAP7, and Flag-tagged-AKAP7$^{H93A;H185R}$ were transfected using Lipofectamine 2000. After 16 h, cells were mock transfected or transfected with poly(rI) · poly(rC) (pIC) (EMD Biosciences) at 1 μg/well for 3 h. The cells were washed with

phosphate-buffered saline (PBS), lysed in buffer (50 mM Tris-HCl, pH 7.2, 0.15 M NaCl, 1% NP-40, 200 μM sodium orthovanadate, 2 mM EDTA, 5 mM $MgCl_2$, 5 mM DTT) and heated to 95°C for 7 min. Lysates were centrifuged for 10 min at 14,000 × *g* at room temperature, and supernatants were passed through Microcon centrifugal filters with a molecular mass cutoff of 3 kDa (Millipore Corporation) for 45 min at 11,000 × *g*. Levels of 2-5A were determined by RNase L-based FRET assays in comparison to a standard curve of authentic (2′-5′)p_3A_3 as we described previously (20).

Viral growth kinetics. Viral growth curves were determined by infecting B6 or *Rnasel*$^{-/-}$ BMM with each virus at an MOI of 1 PFU/cell. After a 1-h incubation, the cells were washed with PBS and cultured with DMEM supplemented with 10% FBS. Culture supernatants were collected at 6, 9, 12, and 24 h postinfection, and virus titers were determined by plaque assays on L2 cells (56).

RNA chip analysis. For analysis of rRNA integrity, total cellular RNA was isolated at 10 h postinfection with the RNeasy kit (QIAGEN). RNA was quantified with a NanoDrop analyzer, and equal quantities of RNA were resolved on RNA chips using an Agilent 2100 bioanalyzer (28).

Immunofluorescence assays. 17Cl-1 cells or B6 BMM were infected with each virus at an MOI of 1. At 9 h postinfection, cells were fixed with 4% paraformaldehyde in PBS, followed by blocking with 2% bovine serum albumin (BSA) and 0.5% Triton X-100 in PBS, and incubated with primary antibodies for 1 h and then with secondary antibodies for 1 h. Cell were stained with DAPI (4′,6-diamidino-2-phenylindole; Molecular Probes, Eugene, OR) and visually analyzed by using an Olympus IX81 inverted fluorescence microscope and associated SlideBook 5.0 software. 293T cells were transfected using Lipofectamine 2000 with an empty lentivector or a lentivector containing cDNA to AKAP7 or AKAP7^{CD}, together with a plasmid expressing VSV G envelope protein (from a pCMV vector) and a pCMV dR8.2 packaging plasmid. Cells were selected with 3 μg/ml puromycin to generate stably expressing cell lines. 293T cell lines were plated on sterile coverslips at 2 × 10^5 cells/well in six-well plates. After 24 h, the cells were washed with PBS, fixed with 4% paraformaldehyde in PBS for 20 min, blocked with 1% BSA and 0.3% Triton X-100 in PBS for 2 h, and incubated with primary anti-AKAP7^{CD} antibody peptide A at a 1:100 dilution at 4°C for 16 h. The cells were washed three times with PBS, probed with secondary Alexa Fluor 488 goat anti-rabbit antibody at a 1:500 dilution, and stained with Vectashield mounting medium with DAPI. Images were collected using an HCX PL APO 63×/1.4-numerical-aperture (NA) oil immersion objective on a Leica SP2 confocal microscope (Leica Microsystems, GmbH, Wetzlar, Germany).

Western blotting. Proteins in cell lysates were separated in 12.5% SDS-polyacrylamide gels and transferred to polyvinylidene difluoride (PVDF) membranes. Membranes were blocked and probed with the antibodies described above and developed using Amersham ECL Western blotting detection reagent (GE Healthcare) and X-ray film (Fig. 1G and 3C) or using Western Lightning Plus-ECL enhanced-chemiluminescence substrate (PerkinElmer), and proteins were detected under an Intelligent dark box II (Fujifilm) (Fig. 2B). As controls for loading and transfer, the blots were probed with anti-glyceraldehyde-3-phosphate dehydrogenase (GAPDH) or anti-β-actin.

Animal experiments. Four-week-old B6 or *Rnasel*$^{-/-}$ mice were anesthetized with isoflurane (IsoFlo; Abbott Laboratories) and inoculated intrahepatically with each virus (2,000 PFU/mouse) in 50 μl of PBS containing 0.75% BSA. At 5 days postinfection, the mice were sacrificed and perfused with PBS. The livers were removed, homogenized, and titrated by plaque assays on L2 cells as previously described (57). All mouse experiments were reviewed and approved by the University of Pennsylvania IACUC.

Statistical analysis. A two-tailed *t* test was performed to determine statistical significance, and the *P* values are shown in Fig. 4. Data were analyzed with GraphPad Prism software (GraphPad Software, Inc., CA).

SUPPLEMENTAL MATERIAL

Supplemental material for this article may be found at http://mbio.asm.org/lookup/suppl/doi:10.1128/mBio.01312-14/-/DCSupplemental.

Figure S1, PDF file, 0.7 MB.
Figure S2, PDF file, 2 MB.
Figure S3, PDF file, 2.4 MB.

ACKNOWLEDGMENTS

We thank Meredith Bond and George R. Stark (Cleveland, OH), Carolina Lopez and Serge Fuchs (Philadelphia, PA), and G. Stanley McKnight and Brian W. Jones (Seattle, WA) for comments made during preparation of the manuscript.

This work was supported by National Institutes of Health grant RO1 AI104887 (to R.H.S. and S.R.W.).

REFERENCES

1. **Alexander WS, Hilton DJ.** 2004. The role of suppressors of cytokine signaling (SOCS) proteins in regulation of the immune response. Annu. Rev. Immunol. **22:**503–529. http://dx.doi.org/10.1146/annurev.immunol.22.091003.090312.
2. **Randall RE, Goodbourn S.** 2008. Interferons and viruses: an interplay between induction, signalling, antiviral responses and virus countermeasures. J. Gen. Virol. **89:**1–47. http://dx.doi.org/10.1099/vir.0.83391-0.
3. **Silverman RH.** 2007. Viral encounters with 2′,5′-oligoadenylate synthetase and RNase L during the interferon antiviral response. J. Virol. **81:**12720–12729. http://dx.doi.org/10.1128/JVI.01471-07.
4. **Chakrabarti A, Jha BK, Silverman RH.** 2011. New insights into the role of RNase L in innate immunity. J. Interferon Cytokine Res. **31:**49–57. http://dx.doi.org/10.1089/jir.2010.0120.
5. **Silverman RH, Weiss SR.** 2014. Viral phosphodiesterases that antagonize double strand RNA signaling to RNase L by degrading 2-5A. J. Interferon Cytokine Res. **34:**455–463.
6. **Sadler AJ, Williams BR.** 2008. Interferon-inducible antiviral effectors. Nat. Rev. Immunol. **8:**559–568. http://dx.doi.org/10.1038/nri2314.
7. **Zhao L, Jha BK, Wu A, Elliott R, Ziebuhr J, Gorbalenya AE, Silverman RH, Weiss SR.** 2012. Antagonism of the interferon-induced OAS-RNase L pathway by murine coronavirus ns2 protein is required for virus replication and liver pathology. Cell Host Microbe **11:**607–616. http://dx.doi.org/10.1016/j.chom.2012.04.011.
8. **Zhang R, Jha BK, Ogden KM, Dong B, Zhao L, Elliott R, Patton JT, Silverman RH, Weiss SR.** 2013. Homologous 2′,5′-phosphodiesterases from disparate RNA viruses antagonize antiviral innate immunity. Proc. Natl. Acad. Sci. U. S. A. **110:**13114–13119. http://dx.doi.org/10.1073/pnas.1306917110.
9. **Mazumder R, Iyer LM, Vasudevan S, Aravind L.** 2002. Detection of novel members, structure-function analysis and evolutionary classification of the 2H phosphoesterase superfamily. Nucleic Acids Res. **30:**5229–5243. http://dx.doi.org/10.1093/nar/gkf645.
10. **Arn EA, Abelson JN.** 1996. The 2′-5′ RNA ligase of Escherichia coli. Purification, cloning, and genomic disruption. J. Biol. Chem. **271:**31145–31153. http://dx.doi.org/10.1074/jbc.271.49.31145.
11. **Snijder EJ, Bredenbeek PJ, Dobbe JC, Thiel V, Ziebuhr J, Poon LL, Guan Y, Rozanov M, Spaan WJ, Gorbalenya AE.** 2003. Unique and conserved features of genome and proteome of SARS-coronavirus, an early split-off from the Coronavirus group 2 lineage. J. Mol. Biol. **331:**991–1004.
12. **Roth-Cross JK, Stokes H, Chang G, Chua MM, Thiel V, Weiss SR, Gorbalenya AE, Siddell SG.** 2009. Organ-specific attenuation of murine hepatitis virus strain A59 by replacement of catalytic residues in the putative viral cyclic phosphodiesterase ns2. J. Virol. **83:**3743–3753. http://dx.doi.org/10.1128/JVI.02203-08.
13. **Welch EJ, Jones BW, Scott JD.** 2010. Networking with AKAPs: context-dependent regulation of anchored enzymes. Mol. Interv. **10:**86–97. http://dx.doi.org/10.1124/mi.10.2.6.
14. **Mauban JR, O'Donnell M, Warrier S, Manni S, Bond M.** 2009. AKAP-scaffolding proteins and regulation of cardiac physiology. Physiology (Bethesda) **24:**78–87. http://dx.doi.org/10.1152/physiol.00041.2008.
15. **McConnachie G, Langeberg LK, Scott JD.** 2006. AKAP signaling complexes: getting to the heart of the matter. Trends Mol. Med. **12:**317–323. http://dx.doi.org/10.1016/j.molmed.2006.05.008.
16. **Diviani D, Dodge-Kafka KL, Li J, Kapiloff MS.** 2011. A-kinase anchoring proteins: scaffolding proteins in the heart. Am. J. Physiol. Heart Circ. Physiol. **301:**H1742–H1753. http://dx.doi.org/10.1152/ajpheart.00569.2011.

17. **Dodge KL, Khouangsathiene S, Kapiloff MS, Mouton R, Hill EV, Houslay MD, Langeberg LK, Scott JD.** 2001. mAKAP assembles a protein kinase A/PDE4 phosphodiesterase cAMP signaling module. EMBO J. **20:**1921–1930. http://dx.doi.org/10.1093/emboj/20.8.1921.
18. **Gold MG, Smith FD, Scott JD, Barford D.** 2008. AKAP18 contains a phosphoesterase domain that binds AMP. J. Mol. Biol. **375:**1329–1343. http://dx.doi.org/10.1016/j.jmb.2007.11.037.
19. **Jones BW, Brunet S, Gilbert ML, Nichols CB, Su T, Westenbroek RE, Scott JD, Catterall WA, McKnight GS.** 2012. Cardiomyocytes from AKAP7 knockout mice respond normally to adrenergic stimulation. Proc. Natl. Acad. Sci. U. S. A. **109:**17099–17104. http://dx.doi.org/10.1073/pnas.1215219109.
20. **Thakur CS, Xu Z, Wang Z, Novince Z, Silverman RH.** 2005. A convenient and sensitive fluorescence resonance energy transfer assay for RNase L and 2′,5′ oligoadenylates. Methods Mol. Med. **116:**103–113.
21. **Baumal R, Law J, Buick RN, Kahn H, Yeger H, Sheldon K, Colgan T, Marks A.** 1986. Monoclonal antibodies to an epithelial ovarian adenocarcinoma: distinctive reactivity with xenografts of the original tumor and a cultured cell line. Cancer Res. **46:**3994–4000.
22. **Kerr IM, Brown RE, Hovanessian AG.** 1977. Nature of inhibitor of cell-free protein synthesis formed in response to interferon and double-stranded RNA. Nature **268:**540–542. http://dx.doi.org/10.1038/268540a0.
23. **Yount B, Denison MR, Weiss SR, Baric RS.** 2002. Systematic assembly of a full-length infectious cDNA of mouse hepatitis virus strain A59. J. Virol. **76:**11065–11078. http://dx.doi.org/10.1128/JVI.76.21.11065-11078.2002.
24. **Brown RL, August SL, Williams CJ, Moss SB.** 2003. AKAP7gamma is a nuclear RI-binding AKAP. Biochem. Biophys. Res. Commun. **306:**394–401. http://dx.doi.org/10.1016/S0006-291X(03)00982-3.
25. **Zhao L, Rose KM, Elliott R, Van Rooijen N, Weiss SR.** 2011. Cell-type-specific type I interferon antagonism influences organ tropism of murine coronavirus. J. Virol. **85:**10058–10068. http://dx.doi.org/10.1128/JVI.05075-11.
26. **Silverman RH, Skehel JJ, James TC, Wreschner DH, Kerr IM.** 1983. rRNA cleavage as an index of ppp(A2′p)nA activity in interferon-treated encephalomyocarditis virus-infected cells. J. Virol. **46:**1051–1055.
27. **Wreschner DH, James TC, Silverman RH, Kerr IM.** 1981. Ribosomal RNA cleavage, nuclease activation and 2-5A(ppp(A2′p)nA) in interferon-treated cells. Nucleic Acids Res. **9:**1571–1581. http://dx.doi.org/10.1093/nar/9.7.1571.
28. **Xiang Y, Wang Z, Murakami J, Plummer S, Klein EA, Carpten JD, Trent JM, Isaacs WB, Casey G, Silverman RH.** 2003. Effects of RNase L mutations associated with prostate cancer on apoptosis induced by 2′,5′-oligoadenylates. Cancer Res. **63:**6795–6801.
29. **Williams BR, Kerr IM, Gilbert CS, White CN, Ball LA.** 1978. Synthesis and breakdown of pppA2′p5′A2′p5′A and transient inhibition of protein synthesis in extracts from interferon-treated and control cells. Eur. J. Biochem. **92:**455–462. http://dx.doi.org/10.1111/j.1432-1033.1978.tb12767.x.
30. **Trujillo MA, Barbet J, Cailla HL.** 1988. Mechanisms of degradation of 2′-5′ oligoadenylates. Biochimie **70:**1733–1744. http://dx.doi.org/10.1016/0300-9084(88)90032-6.
31. **Dong B, Xu L, Zhou A, Hassel BA, Lee X, Torrence PF, Silverman RH.** 1994. Intrinsic molecular activities of the interferon-induced 2-5A-dependent RNase. J. Biol. Chem. **269:**14153–14158.
32. **Cruz JL, Sola I, Becares M, Alberca B, Plana J, Enjuanes L, Zuñiga S.** 2011. Coronavirus gene 7 counteracts host defenses and modulates virus virulence. PLoS Pathog. **7:**e1002090.
33. **Kubota K, Nakahara K, Ohtsuka T, Yoshida S, Kawaguchi J, Fujita Y, Ozeki Y, Hara A, Yoshimura C, Furukawa H, Haruyama H, Ichikawa K, Yamashita M, Matsuoka T, Iijima Y.** 2004. Identification of 2′-phosphodiesterase, which plays a role in the 2-5-A system regulated by interferon. J. Biol. Chem. **279:**37832–37841. http://dx.doi.org/10.1074/jbc.M400089200.
34. **Poulsen JB, Andersen KR, Kjaer KH, Durand F, Faou P, Vestergaard AL, Talbo GH, Hoogenraad N, Brodersen DE, Justesen J, Martensen PM.** 2011. Human 2′-phosphodiesterase localizes to the mitochondrial matrix with a putative function in mitochondrial RNA turnover. Nucleic Acids Res. **39:**3754–3770. http://dx.doi.org/10.1093/nar/gkq1282.
35. **Rorbach J, Nicholls TJ, Minczuk M.** 2011. PDE12 removes mitochondrial RNA poly(A) tails and controls translation in human mitochondria. Nucleic Acids Res. **39:**7750–7763. http://dx.doi.org/10.1093/nar/gkr470.
36. **Poulsen JB, Andersen KR, Kjaer KH, Vestergaard AL, Justesen J, Martensen PM.** 2012. Characterization of human phosphodiesterase 12 and identification of a novel 2′-5′ oligoadenylate nuclease—the ecto-nucleotide pyrophosphatase/phosphodiesterase 1. Biochimie **94:**1098–1107. http://dx.doi.org/10.1016/j.biochi.2012.01.012.
37. **Hovanessian AG, Laurent AG, Chebath J, Galabru J, Robert N, Svab J.** 1987. Identification of 69-kd and 100-kd forms of 2-5A synthetase in interferon-treated human cells by specific monoclonal antibodies. EMBO J. **6:**1273–1280.
38. **Chebath J, Benech P, Hovanessian A, Galabru J, Revel M.** 1987. Four different forms of interferon-induced 2′,5′-oligo(A) synthetase identified by immunoblotting in human cells. J. Biol. Chem. **262:**3852–3857.
39. **Shanks MO, Lund LM, Manni S, Russell M, Mauban JR, Bond M.** 2012. Chromodomain helicase binding protein 8 (Chd8) is a novel A-kinase anchoring protein expressed during rat cardiac development. PLoS One **7:**e46316. http://dx.doi.org/10.1371/journal.pone.0046316.
40. **Wilhelmsen KC, Leibowitz JL, Bond CW, Robb JA.** 1981. The replication of murine coronavirus in enucleated cells. Virology **110:**225–230. http://dx.doi.org/10.1016/0042-6822(81)90027-1.
41. **Nilsen TW, Baglioni C.** 1979. Mechanism for discrimination between viral and host mRNA in interferon-treated cells. Proc. Natl. Acad. Sci. U. S. A. **76:**2600–2604. http://dx.doi.org/10.1073/pnas.76.6.2600.
42. **Reid TR, Hersh CL, Kerr IM, Stark GR.** 1984. Analysis of 2′,5′-oligoadenylates in cells and tissues. Anal. Biochem. **136:**136–141. http://dx.doi.org/10.1016/0003-2697(84)90315-4.
43. **Ontiveros E, Kuo L, Masters PS, Perlman S.** 2001. Inactivation of expression of gene 4 of mouse hepatitis virus strain JHM does not affect virulence in the murine CNS. Virology **289:**230–238. http://dx.doi.org/10.1006/viro.2001.1167.
44. **Hagemeijer MC, Vonk AM, Monastyrska I, Rottier PJ, de Haan CA.** 2012. Visualizing coronavirus RNA synthesis in time using click chemistry. J. Virol. **86:**5808–5816. http://dx.doi.org/10.1128/JVI.07207-11.
45. **Knoops K, Kikkert M, Worm SH, Zevenhoven-Dobbe JC, van der Meer Y, Koster AJ, Mommaas AM, Snijder EJ.** 2008. SARS-coronavirus replication is supported by a reticulovesicular network of modified endoplasmic reticulum. PLoS Biol. **6:**e226. http://dx.doi.org/10.1371/journal.pbio.0060226.
46. **Wyatt RG, James WD, Bohl EH, Theil KW, Saif LJ, Kalica AR, Greenberg HB, Kapikian AZ, Chanock RM.** 1980. Human rotavirus type 2: cultivation *in vitro*. Science **207:**189–191. http://dx.doi.org/10.1126/science.6243190.
47. **Lai MM.** 1990. Coronavirus: organization, replication and expression of genome. Annu. Rev. Microbiol. **44:**303–333. http://dx.doi.org/10.1146/annurev.mi.44.100190.001511.
48. **Luytjes W, Bredenbeek PJ, Noten AF, Horzinek MC, Spaan WJ.** 1988. Sequence of mouse hepatitis virus A59 mRNA 2: indications for RNA recombination between coronaviruses and influenza C virus. Virology **166:**415–422. http://dx.doi.org/10.1016/0042-6822(88)90512-0.
49. **Caamaño J, Alexander J, Craig L, Bravo R, Hunter CA.** 1999. The NF-kappa B family member RelB is required for innate and adaptive immunity to Toxoplasma gondii. J. Immunol. **163:**4453–4461.
50. **Zhou A, Paranjape J, Brown TL, Nie H, Naik S, Dong B, Chang A, Trapp B, Fairchild R, Colmenares C, Silverman RH.** 1997. Interferon action and apoptosis are defective in mice devoid of 2′,5′-oligoadenylate-dependent RNase L. EMBO J. **16:**6355–6363. http://dx.doi.org/10.1093/emboj/16.21.6355.
51. **Leitner WW, Hwang LN, deVeer MJ, Zhou A, Silverman RH, Williams BR, Dubensky TW, Ying H, Restifo NP.** 2003. Alphavirus-based DNA vaccine breaks immunological tolerance by activating innate antiviral pathways. Nat. Med. **9:**33–39.
52. **Campeau E, Ruhl VE, Rodier F, Smith CL, Rahmberg BL, Fuss JO, Campisi J, Yaswen P, Cooper PK, Kaufman PD.** 2009. A versatile viral system for expression and depletion of proteins in mammalian cells. PLoS One **4:**e6529. http://dx.doi.org/10.1371/journal.pone.0006529.
53. **Stewart SA, Dykxhoorn DM, Palliser D, Mizuno H, Yu EY, An DS, Sabatini DM, Chen IS, Hahn WC, Sharp PA, Weinberg RA, Novina CD.** 2003. Lentivirus-delivered stable gene silencing by RNAi in primary cells. RNA **9:**493–501. http://dx.doi.org/10.1261/rna.2192803.
54. **Sperry SM, Kazi L, Graham RL, Baric RS, Weiss SR, Denison MR.** 2005. Single-amino-acid substitutions in open reading frame (ORF) 1b-nsp14 and ORF 2a proteins of the coronavirus mouse hepatitis virus are attenuating in mice. J. Virol. **79:**3391–3400. http://dx.doi.org/10.1128/JVI.79.6.3391-3400.2005.
55. **Molinaro RJ, Jha BK, Malathi K, Varambally S, Chinnaiyan AM,**

Silverman RH. 2006. Selection and cloning of poly(rC)-binding protein 2 and Raf kinase inhibitor protein RNA activators of 2′,5′-oligoadenylate synthetase from prostate cancer cells. Nucleic Acids Res. **34:**6684–6695. http://dx.doi.org/10.1093/nar/gkl968.

56. **Hingley ST, Gombold JL, Lavi E, Weiss SR.** 1994. MHV-A59 fusion mutants are attenuated and display altered hepatotropism. Virology **200:** 1–10. http://dx.doi.org/10.1006/viro.1994.1156.
57. **Gombold JL, Hingley ST, Weiss SR.** 1993. Fusion-defective mutants of mouse hepatitis virus A59 contain a mutation in the spike protein cleavage signal. J. Virol. **67:**4504–4512.